Evaluation of a Locus of Azeotropes by Molecular Simulation

Sandeep P. Pandit and David A. Kofke
Dept. of Chemical Engineering, State University of New York at Buffalo, Buffalo, NY 14260

The technique proposed here for the evaluation of azeotrope lines by molecular simulation builds on ideas used to devise the Gibbs-Duhem integration (GDI) technique for evaluating phase equilibria by molecular simulation. Beginning with a known azeotropic state point, the method integrates a differential equation for the locus of azeotropes with a single semigrand-ensemble molecular simulation performed at each integration state point. Unlike the standard GDI method, fluctuation quantities are needed to conduct the integration. Although these quantities are measured less precisely than simple ensemble averages, the integration is not adversely affected by this difficulty. The method is demonstrated by applying to three model Lennard-Jones binaries. Among these mixtures is one in which the molecular diameter of one species is varied along the azeotrope line. This application shows how details of the intermolecular interactions affect azeotropic behavior. Such an understanding might be useful in formulating additives to break an azeotrope.

Introduction

Molecular simulation is a tool that permits exact evaluation of the bulk thermodynamic properties of systems that are defined in terms of a molecular model (Allen and Tildesley, 1987; Frenkel and Smit, 1996). The physical principles underlying molecular simulation have been in place for much of this century, and the basic approach to the calculation is in many ways unchanged since the advent of molecular simulation in the 1950s, although very important advances in methodology have been made. By the 1980s, molecular simulation had begun to establish itself as a central element of research in chemical engineering thermodynamics. Not surprisingly, from this period onward, substantial advances have been made in the ability of molecular simulation to study systems and phenomena of chemical engineering interest. Examples include (Deem, 1998) zeolites, polymers, biomaterials, adsorption, catalysis, and phase equilibria.

Phase equilibrium is a phenomenon of great importance to chemical engineering practice, and its quantitative prediction and characterization occupy the efforts of a great many researchers and practitioners. Molecular simulation is now routinely applied to evaluate the phase behavior properties of

molecular model systems, but this is so only because of methodological advances made over the past decade. Principal among these is the invention of the Gibbs ensemble method by Panagiotopoulos (1987). In a Gibbs ensemble simulation, the two coexisting phases are simulated simultaneously, in a way that couples them thermodynamically but not physically. Two simulation volumes are used, but the molecules within each do not interact directly with those in the other phase. As a consequence, there is no interface between the phases, and many problems connected with the simulation of interfacial systems are eliminated. Instead, thermodynamic coupling is introduced by permitting the systems to exchange volume and mass, such that the following formulas are obeyed

$$N^{\mathrm{I}} + N^{\mathrm{II}} = N$$
$$V^{\mathrm{I}} + V^{\mathrm{II}} = V \tag{1}$$

Here N^{I} and N^{II} represent the numbers of molecules in phases I and II, respectively, while V^{I} and V^{II} are the corresponding volumes. These values fluctuate during the course of the simulation, as molecules and volume are traded back and forth between the phases. However, the total volume V and total number of molecules N are unchanged throughout

the simulation. Variations of this algorithm are used, particularly for mixtures. These instances notwithstanding, the Gibbs ensemble simulation is very much like the traditional flash calculation of chemical engineering thermodynamics.

The Gibbs ensemble method suffers from certain limitations associated with its need to exchange molecules between the phases. For dense phases or for complex molecules, it can be difficult or even statistically impossible to insert a molecule into one phase from the other. Also, the simulation of phase equilibria involving solids is nearly impossible via the Gibbs ensemble method. Simulations are performed using periodic boundary conditions, for which defect-free crystal lattices can be constructed using only specific numbers of molecules (for example, 32, 64, 108, 256, and so on for a *fcc* lattice). Since the equilibrium number of molecules in each phase is unknown prior to a Gibbs ensemble simulation (although it can be adjusted with N and V), there is no way to ensure that the proper number will be found in the crystal phase over the duration of the calculation.

The Gibbs-Duhem integration (GDI) method provides an alternative to the Gibbs ensemble for the evaluation of phase equilibria (Kofke, 1993, 1998). Molecule exchanges are required by the Gibbs ensemble to ensure equality of fugacities between the phases. The GDI method establishes this equality instead via the Clapeyron equation (or an appropriate generalization of it). The Clapeyron equation is a differential equation for the variation of the pressure with temperature along the coexistence line (Denbigh, 1971)

$$\frac{dP}{d(1/T)} = -\frac{\Delta H}{R \Delta V} \qquad (2)$$

Here P is the pressure, T is the temperature, H is the enthalpy, and V is the volume; the delta (Δ) indicates a difference between the two coexisting phases (such as $\Delta H = H_{vapor} - H_{liquid}$); R is the gas constant. The Clapeyron equation is derived by equating changes in the chemical potentials of two phases as their temperatures and pressures are changed. The GDI algorithm involves the integration of this equation via a predictor-corrector algorithm with the righthand side of the equation evaluated via isothermal-isobaric simulation of the coexisting phases. Because no particle exchanges are invoked, the GDI method can be applied in situations where the Gibbs ensemble fails, including phase equilibria involving solids. A great variety of extensions of this basic idea are possible by considering integrations other than in the pressure-temperature plane. Integration along the direction of changing mixture composition is routinely accomplished, as are integrations in which coexistence is followed as a parameter of the intermolecular potential is varied. The GDI method and its extensions are the subject of a recent review (Kofke, 1998).

Both the GE and the GDI methods are designed to provide the same type of phase coexistence information obtained from a flash calculation. These methods are very effective at providing liquid and vapor compositions as a function of pressure and temperature, or densities and pressure of pure phases as a function of temperature. However, chemical engineers are often interested in other types of phase behavior, or more precisely, other views of the phase diagram. As molecular models improve and simulation is called upon to provide information now obtained via engineering equations

of state, there will be a growing need to have molecular simulation methods that can provide views of phase equilibria that are practically inaccessible via GE or GDI methods. Developments are under way to address these shortcomings of simulation. Escobedo (1998) has recently presented an approach to calculating dew-bubble curves directly by molecular simulation, and we have reported a similar method (Henning and Kofke, 1999). In these calculations, one is interested in tracing a line in the pressure-temperature plane for which the composition of the vapor (dew calculation) or liquid (bubble calculation) phase in a multicomponent mixture is constant. These types of phase diagrams are important in uncovering retrograde phase behavior. Both the Escobedo approach and our own invoke the basic idea of the GDI method: a differential equation is formulated for the coexistence line, and it is integrated using standard methods, with the "righthand side" evaluated by molecular simulation. Escobedo has pointed out that this approach fits into a hierarchy of generalized "integrations," which are unique to molecular simulation because of the depth of information that can be obtained from a single simulation with due effort. In this sense the histogram reweighting method (Ferrenberg and Swendsen, 1988, 1989; Ferrenberg, Landau et al., 1995; Kiyohara, Gubbins et al. 1997), which has grown in use in recent years, represents a very high-order quadrature approach; it has great accuracy, but limited stability (that is, for a step size that is not too large, it gives essentially exact results, but, for a too-large step, the histograms do not overlap and the method can fail catastrophically).

Azeotropes are phase-coexistence states in which both phases have the same composition. They are a special case of the more general phenomenon of indifferent equilibria, which are characterized by vapor and liquid (or solid) compositions that are co-linear (Haase and Schönert, 1969). Azeotropes, if present, are important "landmarks" on the phase diagram, because they impose constraints on the type of separations that can be achieved with distillation. A systematic approach to synthesis of chemical processing systems begins with the mapping of loci of azeotropes, and design is conducted within this framework (Safrit and Westerberg, 1997). Normally, the loci are evaluated by application of an engineering model (such as a cubic equation of state). As molecular models continue to improve, it is likely that chemical engineers will find them appropriate in a broader range of applications. An important step toward the integration of molecular modeling and plant design is the ability to evaluate azeotropic loci from a molecular model. A methodology is presented and demonstrated for this calculation. Like the new dew-bubble calculation methods, the approach extends the ideas behind the GDI method: a differential equation is formulated for the azeotrope line and a series of molecular simulations is conducted that integrate along the path described by the relation. A less familiar application of this methodology permits study of how azeotropy is influenced by features of the intermolecular potential. Variation of, for example, molecular size or electrostatics can be performed while following the resulting variations in azeotropic state conditions. Such a study might be useful in formulating an additive to break an azeotrope.

The semigrand-ensemble formalism for mixtures is reviewed. This provides the framework for the simulation algo-

rithm. The method is developed and it is demonstrated via application to several simple model mixtures.

Semigrand Ensemble

The semigrand ensemble provides a very convenient formalism for the molecular simulation of mixtures (Briano and Glandt, 1984; Kofke and Glandt, 1987; Kofke, 1998). In its usual formulation, which is the one we apply here, the independent state variables are T and P, the total number of molecules N, and the set of chemical potential differences $\{\Delta\mu_j\}$, where the differences are formed with respect to an arbitrarily chosen reference species, which we will designate as species 1: $\Delta\mu_j \equiv \mu_j - \mu_1$. The fundamental equation for this ensemble is derived by performing the Legendre transform (Callen, 1985) of the isothermal-isobaric ensemble formula, properly recast in terms of the chemical potential differences

$$d(\beta G) = Hd\beta - \beta VdP + \beta\mu_1 dN - \sum_{j=2}^{c} \beta\Delta\mu_j dN_j \quad (3)$$

where G is the Gibbs free energy; for notational convenience, we introduce the reciprocal temperature $\beta = 1/k_B T$, where k_B is the Boltzmann's constant. Legendre transformation yields expressions for the semigrand free energy Y_N of a mixture containing c components

$$Y_N \equiv G - \sum_{j=2}^{c} N_j\Delta\mu_j = N\mu_1 \quad (4a)$$

$$d(\beta Y_N) = Hd\beta + \beta VdP + \beta\mu_1 dN - \sum_{j=2}^{c} N_j d(\beta\Delta\mu_j) \quad (4b)$$

Unlike real systems, the systems modeled in molecular simulations can be varied in ways that go beyond changes in their thermodynamic state. We can adjust parameters of the intermolecular potential, increasing or decreasing the size of molecules, the strength of their interactions, and their electrostatic features. The effect of these changes can be characterized through the familiar thermodynamic formalism such as reviewed above. The intermolecular potential parameter subject to variation takes the role of a thermodynamic field variable, such as the temperature or pressure; it must have the same value at all points in an equilibrated system. The conjugate variable describes how the free energy changes with respect to changes in this potential parameter. Thus, we write

$$d(\beta Y_N) = Hd\beta + \beta VdP + N\chi ds + \beta\mu_1 dN$$
$$- \sum_{j=2}^{c} N_j d(\beta\Delta\mu_j) \quad (5)$$

Here, we let s designate the potential parameter that may be varied, and χ is its thermodynamic conjugate. It is not difficult to show (Kofke, 1998) that χ can be written as the ensemble average of the derivative of the intermolecular potential energy U with respect to s

$$\chi \equiv \left(\frac{\partial\beta\mu_1}{\partial s}\right)_{T,p,N,\Delta\mu_j} = \frac{1}{N}\left\langle\frac{\partial\beta U}{\partial s}\right\rangle \quad (6)$$

A desirable feature of this semigrand ensemble is that the total number of molecules N is an independent quantity, even though no species mole numbers are specified. This outcome is appealing, because it means that a simulation can be conducted in this ensemble without requiring trials in which molecules are inserted in or deleted from the simulation volume. Instead, Monte Carlo simulation trials are conducted in which a randomly selected molecule randomly changes its species identity. The trial is accepted using a criterion that depends on the change in intermolecular energy accompanying the process, as well as on the chemical-potential differences

$$p_{acc} = \min\left\{1, \exp\left[-\beta(U^{new} - U^{old}) + \beta(\Delta\mu^{new} - \Delta\mu^{old})\right]\right\} \quad (7)$$

where new and old indicate values in the previous and the trial states, and the chemical potential differences refer to that for the particle undergoing the identity change. The trial is accepted if p_{acc} is found to be greater than a (pseudo) random number selected uniformly on (0, 1). Details of the process are available elsewhere (Kofke and Glandt, 1988; Mehta and Kofke, 1994; Kofke, 1998; Frenkel and Smit, 1996).

Method

The first step in the formulation of the method is the establishment of a differential equation for the coexistence line. The development of such equations is demonstrated in standard thermodynamics texts (Denbigh, 1971; Modell and Reid, 1983), although the use of the semigrand ensemble, as done here, is atypical. We consider vapor-liquid equilibrium for a two-component mixture. Continuing from the semigrand formalism reviewed in the previous section, we may write the Gibbs-Duhem equation for the mixture in each phase as follows

$$d(\beta\mu_1^L) = h^L d\beta + \beta\nu^L dP + \chi^L ds - X_2 d(\beta\Delta\mu)$$
$$d(\beta\mu_1^V) = h^V d\beta + \beta\nu^V dP + \chi^V ds - Y_2 d(\beta\Delta\mu) \quad (8)$$

The superscripts L and V indicate the liquid and vapor phases, respectively, and we use X_2 and Y_2 to represent the corresponding mole fractions of species 2. Presently, we will focus on developing relations that describe how pressure, temperature, and composition vary along the azeotrope locus. Extensions that consider variations in the intermolecular potential parameter s follow in a straightforward way.

Along any coexistence line, variations in all the field variables must be the same in both phases. In particular, simultaneous changes in T, p, $\Delta\mu$ and/or s must occur in a way that preserves equality of $\beta\mu_1$. Eliminating $d(\beta\mu_1)$ between the equations for each phase results

$$(h^L - h^V)d\beta + \beta(\nu^L - \nu^V)dP + (\chi^L - \chi^V)ds$$
$$- (X_2 - Y_2)d(\beta\Delta\mu) = 0 \quad (9)$$

Of course, along the azeotrope locus the species mole fractions are the same between the phases ($X_2 = Y_2$), so the term

in $d(\beta\Delta\mu)$ drops out. Considering the intermolecular potential unchanged along our path, $ds = 0$ also, we have a simple relation for changes in pressure and temperature along the azeotrope locus

$$\left(\frac{dP^{\text{sat}}}{d\beta}\right)_{\text{azeo}} = -\frac{h^L - h^V}{\beta(\nu^L - \nu^V)} \tag{10}$$

This is the familiar Clapeyron equation that is more commonly encountered when considering P-T changes for a one-species vapor-liquid coexistence.

Along the azeotrope locus, the mixture mole fractions change with pressure and temperature. To ensure that the composition changes identically in the two phases, and the azeotrope condition is maintained, we must also adjust $\beta\Delta\mu$ along the integration path. The governing equation can be obtained by expressing the change in the composition as follows

$$dX_1 = \left(\frac{\partial X_1}{\partial \beta}\right)_{P,\beta\Delta\mu} d\beta + \left(\frac{\partial X_1}{\partial P}\right)_{\beta,\beta\Delta\mu} dP$$
$$+ \left(\frac{\partial X_1}{\partial \beta\Delta\mu}\right)_{P,\beta} d(\beta\Delta\mu)$$

$$dY_1 = \left(\frac{\partial Y_1}{\partial \beta}\right)_{P,\beta\Delta\mu} d\beta + \left(\frac{\partial Y_1}{\partial P}\right)_{\beta,\beta\Delta\mu} dP$$
$$+ \left(\frac{\partial Y_1}{\partial \beta\Delta\mu}\right)_{P,\beta} d(\beta\Delta\mu) \tag{11}$$

Setting these equations equal, we obtain an expression for how $\Delta\mu$ must vary to maintain azeotropy as the temperature is changed

$$\left(\frac{d(\beta\Delta\mu)}{d\beta}\right)_{\text{azeo}} = \frac{\left\{\left(\frac{\partial X_1}{\partial \beta}\right)_{P,\beta\Delta\mu} - \left(\frac{\partial Y_1}{\partial \beta}\right)_{P,\beta\Delta\mu}\right\} + \left\{\left(\frac{\partial X_1}{\partial P}\right)_{\beta,\beta\Delta\mu} - \left(\frac{\partial Y_1}{\partial P}\right)_{\beta,\beta\Delta\mu}\right\}\left(\frac{dP^{\text{sat}}}{d\beta}\right)_{\text{azeo}}}{\left\{\left(\frac{\partial Y_1}{\partial \beta\Delta\mu}\right)_{P,\beta} - \left(\frac{\partial X_1}{\partial \beta\Delta\mu}\right)_{P,\beta}\right\}} \tag{12}$$

Here $dP^{\text{sat}}/d\beta$ is given by Eq. 10, and the other derivatives appearing on the righthand side can be computed by molecular simulation as described in the Appendix. These derivatives involve averages of a different nature than those used in the standard GDI method. The present derivatives are given in terms of "fluctuation" quantities, similar to the heat capacity or the compressibility (McQuarrie, 1976). These quantities are computed as the difference between order-N^2 ensemble averages to yield a quantity of order N. As a consequence, they cannot be obtained as precisely as straightforward averages used to measure the energy or the pressure. One of the objectives in this study is to find whether the imprecision in these quantities causes any undue difficulties in our new algorithm.

The algorithm proceeds as follows. A known azeotropic state point is used to initiate the procedure. A semigrand-ensemble molecular simulation is conducted for the two phases at this state, and averages are recorded necessarily to evaluate the righthand sides of Eqs. 10 and 12. A step $\Delta\beta$ in temperature is taken, and a predictor algorithm is used to estimate P and $\beta\Delta\mu$ at the new temperature. Simulations of the phases are conducted at this new state point, and new averages are recorded for Eqs. 10 and 12. These averages are fed into a corrector algorithm to adjust P and $\beta\Delta\mu$, the simulations continue, and the process repeats to convergence. Details of the predictor/corrector algorithm and updating procedure are largely the same as those used in the standard and well-documented (Kofke, 1998) GDI algorithm, so they will not be repeated here.

It should be noted that the requirement of composition equality is not strictly enforced by the algorithm, and that the procedure is designed to result only in equal ensemble-averaged mole fractions at each state point. Obviously, these averages should be examined to see that the integration indeed follows the azeotropic locus. Deviation of the liquid and vapor compositions from each other indicates an error in the calculation of the chemical potential difference via Eq. 12.

Evaluation of azeotrope loci as a function of an inter-molecular-potential parameter s proceeds as just described, except that the pressure or temperature is held fixed and the governing equations are modified accordingly. For example, if the isothermal variation is of interest, the equation for the change in pressure now takes the form

$$\left(\frac{dP^{\text{sat}}}{ds}\right)_{\beta,\text{azeo}} = -\frac{\Delta x}{\beta\Delta\nu} \tag{13}$$

The change in $\beta\Delta\mu$ with s is given exactly as in Eq. 12, but with s replacing β, and χ replacing h.

Application of Method

We demonstrate the workings of the technique by application to several model binary Lennard-Jones (LJ) mixtures. The size and energy parameters for the like- and unlike-species interactions are summarized in Table 1; we henceforth consider all quantities made dimensionless by the species-1 Lennard-Jones size and energy parameters σ_{11} and ϵ_{11}. The first mixture is similar to one that has served as a prototype for at least three prior studies (Panagiotopoulos et al., 1986, 1988; Mehta and Kofke, 1994); it is a simple, symmetric mixture having identical 1-1 and 2-2 parameters, with an unfavorable 1-2 interaction that gives rise to an azeotrope

Table 1. Lennard-Jones Potential Parameters for the Mixtures Examined in this Work

Mixture	σ_{11}	σ_{12}	σ_{22}	ϵ_{11}	ϵ_{12}	ϵ_{22}
1	1.00	1.05	1.00	1.00	0.90	1.00
2	1.00	1.05	1.15	1.00	0.90	1.00
3	1.00	1.05	variable	1.00	0.90	1.00

at equimolar compositions. These same energy parameters are used also in the other mixtures. However, the components in the second and third mixtures have different sizes and, thus, do not display symmetric phase diagrams. In the third mixture, we examine the effect of the molecular diameter of one species on the phase behavior to demonstrate how azeotropes can be traced with respect to a parameter in the intermolecular potential. Clearly our aim in choosing these simple systems for our illustration is not to improve our understanding of azeotropy, but merely to demonstrate the efficacy of this new tool to characterize azeotropic systems.

In all cases we require an initial azeotropic point to start the integration of pressure with respect to temperature (or size parameter in the case of Mixture 3). This point should also provide the initial chemical potential difference ($\beta\Delta\mu$) as the starting point for integrating Eq. 12 and for the semigrand identity-change acceptance criterion (Eq. 7). Of course, the 1-2 symmetry of Mixture 1 indicates that the azeotrope occurs at a mole fraction of one-half, and that the chemical-potential difference is zero here (however, determination of the azeotropic pressure for a given temperature is not so trivial). In general these features are unknown *a priori* and must be provided by separate simulations. To obtain these data, we conducted standard Gibbs-Duhem integrations in composition (Mehta and Kofke, 1994), beginning from a pure (one-component) Lennard-Jones vapor-liquid coexistence point (pure component 1). This integration provides directly the azeotropic conditions of pressure, composition, and chemical-potential difference for a mixture of given temperature.

The chemical-potential difference can alternatively be obtained during a simulation of the azeotrope, which may be useful if the azeotropic condition is already known even though the chemical potentials are not. The method employs virtual identity change moves according to the formulae of Sindzingre et al. (1987)

$$\Delta\mu^{\text{res}} = \mu_2^{\text{res}} - \mu_1^{\text{res}} = -\beta^{-1}\ln\langle\exp(-\beta\Delta U^{2^+1^-})\rangle_{N_2,N_1}$$

$$= \beta^{-1}\ln\langle\exp(-\beta\Delta U^{1^+2^-})\rangle_{N_2,N_1} \qquad (14)$$

where the res superscript refers to the chemical potential for the component in excess of its value in an ideal-gas mixture of the same composition and density. $\Delta U^{i^+j^-}$ refers to the internal energy change associated with changing a particle of species j to that of species i. It should be emphasized that these moves are "virtual," and the particles are changed back to their original species identity before the simulation continues, so both formulas may be applied in the same simulation. If the results are significantly different for the different identity change moves, then one needs to rely on the results supplied by the move in which a smaller particle is changed to a larger one (Kofke and Cummings, 1997).

Simulations were conducted using 108 LJ particles in each phase; 5,000 predictor cycles, 6 to 8 corrector iterations (with 5,000 cycles per iteration) and 10,000 to 15,000 production cycles were performed for each integration step. The cutoff radius of interaction was set constant for each simulation with a value of $2.75\sigma_{11}$, and the usual correction for potential truncation was applied (Allen and Tildesley, 1987). To verify the results for the azeotrope integrations, we performed a (much lengthier) set of GDI calculations at each temperature

to trace the complete coexistence using equispaced value of ξ_2, except in mixture 2 where a finer step size was needed in the vicinity of the azeotrope to get the azeotropic pressure and composition used as the starting point for the pressure-temperature integration.

Results for symmetric mixture 1

The symmetric Mixture 1 provides our first demonstration of the algorithm. The azeotrope always occurs at the equimolar composition and $\beta\Delta\mu = 0$ for all temperatures along the azeotrope, so the test probes mainly the ability of the algorithm to trace the azeotropic pressure as a function of temperature. However, since the azeotropic mole fraction is known exactly, this calculation also gives some indication of the precision we should expect in the semigrand-ensemble averaged mole fractions. The azeotropic point at the reduced temperature of 1.10 was used as the initial state point for the integration, which itself was established by a GDI from the coexistence point of the pure LJ fluid at the same temperature (Kofke, 1993). The azeotrope integration then proceeded in three steps to $T^* = 0.90$. The results are presented in Figure 1, and the azeotrope data are tabulated in Table 2. The agreement with the full pressure-composition data is excellent. The mole fractions are very close (usually well within 1%) to the correct equimolar values.

Results for asymmetric mixture 2

Integration for Mixture 2 began at reduced temperature $T^* = 1.10$ and proceeded in four steps to $T^* = 0.90$. The results are shown in Figure 2 and Table 3. The azeotropic condition of equal mole fractions is satisfied well between the phases, and the vapor and liquid mole fractions are within 1% of each other at all temperatures. Comparison with the independently measured phase diagrams shows very good agreement for the azeotropic conditions. Another study of a similar mixture showed equally good agreement between the azeotrope measurements (Pandit, 1998). One azeotropic datum from Mixture 3 coincides with the conditions studied here for Mixture 2, and is presented on the figure. This comparison is discussed below.

Tracking azeotropes as a function of the particle-size parameter

The two foregoing mixtures provide an incomplete test and demonstration of the proposed algorithm. Mixture 1 exhibits no variation in the azeotropic composition, and Mixture 2 shows almost none. The ability to track changes in azeotropic composition is a key element of the algorithm, and it is important to test that this can be done. The molecular size parameters influence greatly the symmetry of the phase diagram, and thus have a large effect on the azeotropic composition. In this example we consider how the azeotropic conditions (pressure and mole fraction) change with the diameter of one of the species at a constant temperature. This example has the added advantage of demonstrating an integration path in which an intermolecular-potential parameter is changed.

The particle size for 2-2 interactions (σ_{22}) is our potential parameter s (cf. Eq. 5) and was varied from 1.00 to 1.20 in
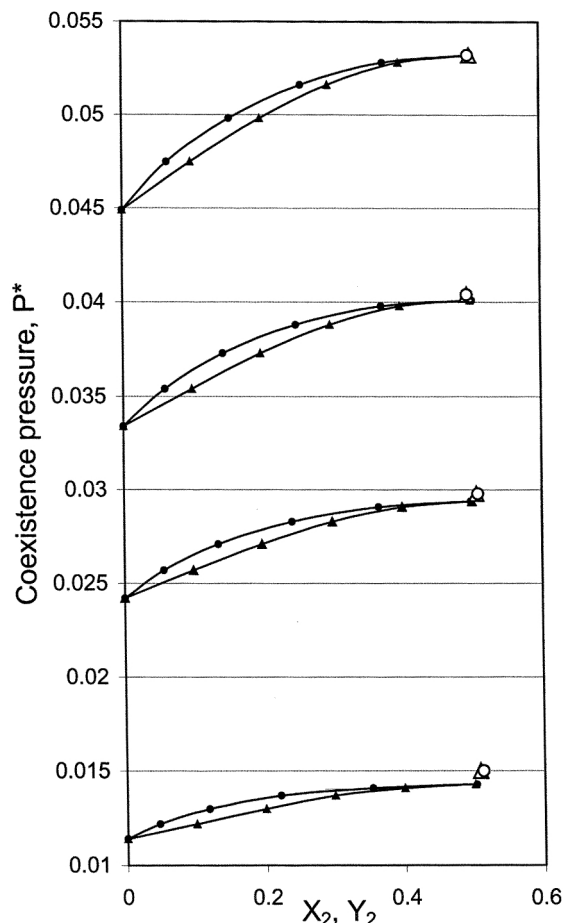
Figure 1. Pressure-composition coexistence diagram for the symmetric mixture 1.

Pressure is reduced by the Lennard-Jones parameters of species 1. Small filled circles and triangles are data determined by a standard semigrand-ensemble Gibbs-Duhem integration. Large open circles (liquid) and triangles (vapor) describe the pressure-composition conditions for the azeotrope, as determined by the proposed technique. Starting from the top, temperatures for the data sets are $T^* =$ 1.10, 1.05, 1.00, and 0.90, respectively. Coexistence diagram is symmetric with respect to exchange of species 1 and 2 mole fractions, so only half of the complete diagram is presented.

four steps. The thermodynamic conjugate χ is evaluated by the simulation via the ensemble average given in Eq. 6. All the simulations were run at a (reduced) temperature T^* of 1.10. The integration starts from $\sigma_{22} = 1.00$, which is Mixture
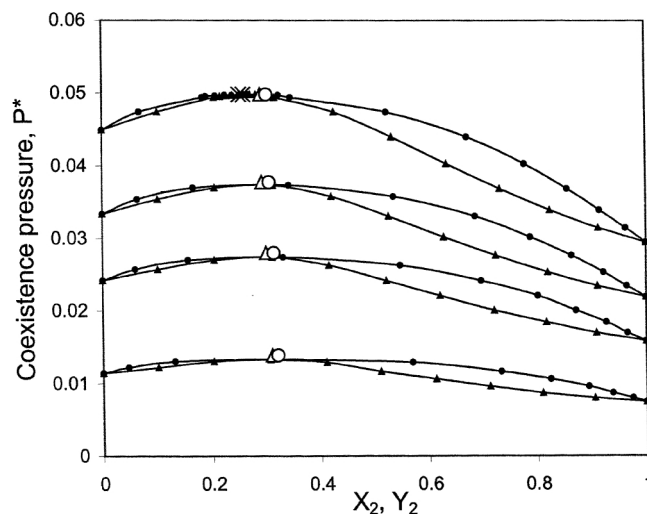

Figure 2. Pressure-composition diagram for the asymmetric mixture 2.

Symbols are as described in Figure 1. Temperatures for the curves are, from top to bottom, $T^* = 1.10$, 1.05, 1.00, 0.90. Crosses on the $T^* = 1.10$ series describe azeotrope as determined from integration of Mixture 3.

1 and thus forms a symmetric phase diagram with azeotropic mole fraction of 0.5 and $\beta\Delta\mu = 0$. However, as integration proceeds to other values of σ_{22}, the value of $\beta\Delta\mu$ becomes non-zero and there is a change in the azeotropic composition.

The results are presented in Figure 3 and Table 4. The integration data agree very nicely with the independently-measured phase diagrams. The azeotropic mole fraction varies considerably, from 0.5 to 0.21, but tracks the pressure maximum in the phase diagram very well. The semigrand-ensemble averaged liquid and vapor mole fractions again agree with each other to within about 1%. The results indicate that the need to use fluctuation averages to perform the integration does not seriously hinder the algorithm.

This integration for Mixture 3 crosses results from Mixture 2 at the conditions $T^* = 1.10$, $\sigma_{22} = 1.15$. It is interesting to compare the azeotrope given by the two calculations, which describe two very different pathways. We find that the azeotropic pressures are in perfect agreement, but the compositions differ markedly (0.26 vs. 0.30). The discrepancy seems to have its origins not in the integration, but in the choice of the azeotropic composition for the Mixture 2 series. We see from Figure 2 that the flatness of the $T^* = 1.10$ coex-

Table 2. Azeotrope Pressure and Composition as a Function of Temperature for Symmetric Mixture 1*

P^*_{azeo}	T^*	Y_2	X_2
0.0532	1.10	0.5002	0.4981
0.0404	1.05	0.4950	0.4950
0.0298	1.00	0.5060	0.5083
0.0150	0.90	0.5078	0.5125

*Pressure and temperature are made dimensionless by the Lennard-Jones parameters of component 1; Y_2 and X_2 are the vapor and liquid mole fractions (respectively) of component 2 at the azeotrope.

Table 3. Azeotrope Pressure and Composition as a Function of Temperature for Asymmetric Mixture 2*

P^*_{azeo}	T^*	Y_2	X_2
0.0498	1.10	0.2906	0.3018
0.0378	1.05	0.2929	0.3064
0.0280	1.00	0.3001	0.3144
0.0139	0.90	0.3105	0.3210

*Pressure and temperature are made dimensionless by the Lennard-Jones parameters of component 1; Y_2 and X_2 are the vapor and liquid mole fractions (respectively) of component 2 at the azeotrope.
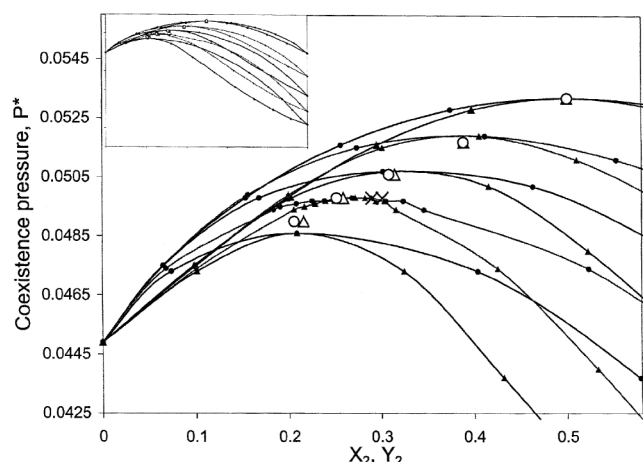
Figure 3. Pressure-composition diagram for mixture 3 for $T^* = 1.10$.

Symbols are as described in Figure 1. Species-2 diameters for the curves are, from top to bottom, $\sigma_{22} = 1.00$, 1.05, 1.10, 1.15, and 1.20. Crosses on the $\sigma_{22} = 1.15$ series describe azeotrope as determined from integration of Mixture 2. Inset shows the complete coexistence curves, while main figure expands the region of the azeotrope locus.

istence line introduces some uncertainty in the identification of the azeotropic composition; it seems (perhaps in retrospect) that the point taken as the azeotrope is not at the maximum of the curve since the step size was not small enough to identify the azeotropic point with a high degree of accuracy. The Mixture 3 calculation does not suffer this problem, because it begins with a symmetric mixture for which the azeotropic composition is known exactly. We performed the Mixture 3 series after completing the Mixture 2 calculation, so we did not have this information to guide our determination of the Mixture 2 initial azeotropic composition. Rather than repeat this calculation with the (presumably) corrected initial composition, we leave this as a lesson in the care one must take when attempting to identify the azeotropic composition from a pressure-composition isotherm.

Concluding Remarks

A method has been developed and demonstrated to generate a locus of azeotropes for a mixture, as a function of temperature, pressure, and/or parameters of the intermolecular potential. The method represents an extension of the Gibbs-

Table 4. Azeotrope Pressure and Composition as a Function of Species-2 Diameter σ_{22} for Asymmetric Mixture 3 at a Reduced Temperature $T^* = 1.10$*

P^*	σ_{22}	Y_2	X_2
0.0532	1.00	0.5005	0.5009
0.0517	1.05	0.3899	0.3896
0.0506	1.10	0.3154	0.3088
0.0.498	1.15	0.2595	0.2523
0.0490	1.20	0.2164	0.2063

*All quantities are made dimensionless by the Lennard-Jones parameters of component 1; Y_2 and X_2 are the vapor and liquid mole fractions (respectively) of component 2 at the azeotrope.

Duhem integration algorithm, reformulated to follow a coexistence line in which the compositions of the two coexisting phases are made equal to each other. The simulations are conducted in a semigrand ensemble, and chemical-potential differences input to the simulation are prescribed by the integration of a differential equation that is formulated to ensure composition equality. Unlike the original GDI method, this extension of it requires simulation averages for fluctuation "second-derivative" quantities as inputs to the integration scheme. While measurement of these quantities is inherently less precise than measurements of the more common "first-derivative" quantities, the algorithm is effective nevertheless.

Any new simulation method must pay some consideration to system-size effects. For simple potentials away from a critical point, the first-derivative quantities converge quickly with increasing N; second-derivative quantities converge less so, and, consequently, finite-size effects may become more of an issue in the proposed method then they were with the original GDI method. In the present study we were able to test for finite-size errors via independent measurement of the azeotropes, and did not observe any serious error. However, absent of such confirmation, it is advisable to perform a few calculations at other system sizes, even if only to examine the effect on the second-derivative quantities outside of the integration scheme, to rule out problems of this type. Of course, this caveat applies *a fortiori* when in the vicinity of a critical point, or when dealing with complex fluids such as ionic or macromolecular systems.

The method has been detailed and demonstrated for binary mixtures, but extension to multicomponent mixtures follows in a straightforward way. To do this, one must generate additional equations similar to Eq. 12 for each added component to the mixture, and integrate them along with the other equations to determine all chemical-potential differences used in the semigrand simulations. These equations would be generated by writing extensions of Eq. 11 (incorporating another $d(\beta \Delta \mu)$ term for each species, and writing a set of equations for each added species) and solving them simultaneously for all $\beta \Delta \mu$.

This work demonstrates how molecular simulation can be used to generate specialized views of the phase behavior of model systems, beyond what can be obtained efficiently with existing methods. The approach we develop here is quite general, and may be applied to generate other interesting views of the phase diagram. The first step is the formulation of a differential equation characterizing the path of interest through the phase diagram. The righthand side of the differential equation is evaluated by molecular simulation, and the equation is integrated with a predictor-corrector algorithm. The quantities required from the simulation can sometimes be given as direct simulation averages, but may often require fluctuation averages such as the compressibility. Depending on the choice of ensemble for the simulation, more than one approach can be formulated to yield the same coexistence line. For example, for the present study, we considered an algorithm based on canonical-ensemble simulations, but we found that the derivatives required from the simulation were less conveniently evaluated than those used by the method we presented here. Some thought toward alternatives may prove worthwhile when formulating an approach to generate a new view on the phase diagram.

We close by pointing out a limitation of the general technique that we have advocated here. Critical points and critical lines are important features of the phase diagram, and they are very difficult to study by molecular simulation. Near a critical point, finite-size effects become very significant, and specialized measures are needed to extract infinite-system results from simulation data (Bruce and Wilding, 1992). Clearly, the straightforward ensemble averaging that underlies GDI methods cannot cope with critical phenomena. Nevertheless, it would be highly valuable to have an efficient and reliable means for evaluating critical lines. The ideas presented here could perhaps be combined with finite-size scaling approaches to produce an effective method to this end.

Acknowledgments

Literature Cited

Allen, M. P., and D. J. Tildesley, *Computer Simulation of Liquids*, Clarendon Press, Oxford (1987).

Briano, J. G., and E. D. Glandt, "Statistical Thermodynamics of Polydisperse Fluids," *J. Chem. Phys.*, **80**, 3336 (1984).

Bruce, A. D., and N. B. Wilding, "Scaling Fields and Universality of the Liquid-Gas Critical Point," *Phys. Rev. Lett.*, **68**, 193 (1992).

Callen, H. B., *Thermodynamics and an Introduction to Thermostatics*, Wiley, New York (1985).

Deem, M. W., "Recent Contributions of Statistical Mechanics in Chemical Engineering," *AIChE J.*, **44**, 2569 (1998).

Denbigh, K., *Principles of Chemical Equilibrium*, Cambridge University Press, Cambridge (1971).

Escobedo, F. A., "Novel Pseudoensembles for Simulation of Multicomponent Phase Equilibria," *J. Chem. Phys.*, **108**, 8671 (1998).

Ferrenberg, A. M., et al., "Statistical Errors in Histogram Reweighting," *Phys. Rev. E*, **51**, 5092 (1995).

Ferrenberg, A. M., and R. H. Swendsen, "New Monte Carlo Technique for Studying Phase Transitions," *Phys. Rev. Lett.*, **61**, 2635 (1988).

Ferrenberg, A. M., and R. H. Swendsen, "Optimized Monte Carlo Data Analysis," *Phys. Rev. Lett.*, **63**, 1195 (1989).

Frenkel, D., and B. Smit, *Understanding Molecular Simulation: From Algorithms to Applications*, Academic Press, Boston, MA (1996).

Haase, R., and H. Schönert, *Solid-Liquid Equilibrium*, Pergamon Press, Oxford (1969).

Henning, J., and D. A. Kofke, "Thermodynamic Integration Along Coexistence Lines," *Molecular Dynamics*, P. B. Balbuena and J. Seminario, eds., Elsevier, Amsterdam, (1999).

Kiyohara, K., et al., "Phase Coexistence Properties of Polarizable Stockmayer Fluids," *J. Chem. Phys.*, **106**, 3338 (1997).

Kofke, D. A., "Direct Evaluation of Phase Coexistence by Molecular Simulation via Integration Along the Saturation Line," *J. Chem. Phys*, **98**, 4149 (1993).

Kofke, D. A., "Semigrand Canonical Monte Carlo Simulation. Integration Along Coexistence Lines," *Monte Carlo Methods in Chemistry*, D. M. Ferguson, J. I. Siepmann, and D. G. Truhlar, eds., Wiley, **105** (1998).

Kofke, D. A., and P. T. Cummings, "Quantitative Comparison and Optimization of Methods for Evaluating the Chemical Potential by Molecular Simulation," *Molec. Phys.*, **92**, 973 (1997).

Kofke, D. A., and E. D. Glandt, "Nearly Monodisperse Fluids. I. Monte Carlo Simulations of Lennard-Jones Particles in a Semigrand Ensemble," *J. Chem. Phys.*, **87**, 4881 (1987).

Kofke, D. A., and E. D. Glandt, "Monte Carlo Simulation of Multicomponent Equilibria in a Semigrand Canonical Ensemble," *Molec. Phys.*, **64**, 1105 (1988).

McQuarrie, D. A., *Statistical Mechanics*, Harper and Row, New York (1976).

Mehta, M., and D. A. Kofke, "Coexistence Diagrams of Mixtures by Molecular Simulation," *Chem. Eng. Sci.*, **49**, 2633 (1994).

Modell, M., and R. C. Reid, *Thermodynamics and Its Applications*, Prentice-Hall, Englewood Cliffs, NJ (1983).

Panagiotopoulos, A. Z., "Direct Determination of Phase Coexistence Properties of Fluids by Monte Carlo Simulation in a New Ensemble," *Mol. Phys.*, **61**, 813 (1987).

Panagiotopoulos, A. Z., et al., "Phase Equilibria by Simulation in the Gibbs Ensemble: Alternative Derivation, Generalization and Application to Mixture and Membrane Equilibria," *Mol. Phys.*, **63**, 527 (1988).

Panagiotopoulos, A. Z., et al., "Phase Diagrams of Non-Ideal Fluid Mixtures from Monte Carlo Simulation," *Ind. Eng. Chem. Fundam.*, **25**, 525 (1986).

Pandit, S. P., "Efficient Methods for Calculating Bubble-Dew and Azeotrope Curves by Molecular Simulation," MS Thesis, State University of New York at Buffalo, Buffalo, NY (1998).

Safrit, B. T., and A. W. Westerberg, "Algorithm for Generating the Distillation Regions for Azeotropic Multicomponent Mixtures," *Ind. Eng. Chem. Res.*, **36**, 1827 (1997).

Sindzingre, P., et al., "Partial Enthalpies and Related Quantities from Computer Simulation," *Chem. Phys. Lett.*, **136**, 35 (1987).

Appendix

The derivatives arising in Eq. 12 can be evaluated via the following semigrand-ensemble averages

$$\left(\frac{\partial X_1}{\partial \beta \Delta \mu}\right)_{P,\beta,N} = \frac{1}{N}\left\{\langle N_1 N_2\rangle^L - \langle N_1\rangle^L\langle N_2\rangle^L\right\} \quad (A1)$$

$$\left(\frac{\partial X_1}{\partial P}\right)_{\beta \Delta \mu,\beta,N} = \frac{\beta}{N}\left[\langle V N_2\rangle^L - \langle V\rangle^L\langle N_2\rangle^L\right] \quad (A2)$$

$$\left(\frac{\partial X_1}{\partial \beta}\right)_{\beta \Delta \mu,P,N} = \frac{1}{N}\left[\langle H N_2\rangle^L - \langle H\rangle^L\langle N_2\rangle^L\right] \quad (A3)$$

The study of Mixture 3 requires the following derivative

$$\left(\frac{\partial X_1}{\partial \sigma_{22}}\right)_{\beta,\beta \Delta \mu,P,N} = \langle \chi N_2\rangle^L - \langle \chi\rangle^L\langle N_2\rangle^L \quad (A4)$$

Formulas for Y_1 are identical, except they involve averages taken in the vapor phase.